Active motility and wetting cooperatively regulate liquid-liquid phase separation

Dixi Yang, 1,* Anheng Wang, 2, 3, 4, * Chunming Wang, 2, 3, 4, † Hajime Tanaka, 5, 6, ‡ and Jiaxing Yuan^{1, §}

¹ Advanced Materials Thrust, Function Hub, The Hong Kong University
of Science and Technology (Guangzhou), Guangzhou 511453, China

² Institute of Chinese Medical Sciences & State Key Laboratory of Mechanism and Quality of Chinese Medicine,
University of Macau, Macau SAR 999078, China

³ Department of Pharmaceutical Sciences, Faculty of Health Sciences,
University of Macau, Macau SAR 999078, China

⁴ Zhuhai UM Science and Technology Research Institute,
University of Macau, Hengqin 519031, Guangdong, China

⁵ Research Center for Advanced Science and Technology,
The University of Tokyo, 4-6-1 Komaba, Meguro-ku, Tokyo 153-8904, Japan

⁶ Department of Fundamental Engineering, Institute of Industrial Science,
The University of Tokyo, 4-6-1 Komaba, Meguro-ku, Tokyo 153-8505, Japan
(Dated: November 13, 2025)

Liquid—liquid phase separation of aqueous two-phase system (ATPS) is fundamental across physical and biological sciences. While well understood for passive systems, how this process is regulated by active agents such as motile bacteria remains largely unexplored. By combining experiments on *Pseudomonas aeruginosa* in a prototypical dextran—polyethylene glycol ATPS with hydrodynamic simulations, we show that the interplay between bacterial activity and interfacial wetting gives rise to a robust sequence of nonequilibrium morphologies, including self-spinning droplets, elongated droplet chains, branched capillary-like clusters, and highly deformed droplets. We find that activity plays a dual role in coarsening kinetics: it suppresses coarsening through hydrodynamically driven, activity-induced droplet rotation, yet accelerates it when dextran is the minority phase, where wetting-mediated attraction governs bacterial aggregation. These findings reveal a generic physical mechanism through which motility and wetting cooperatively control phase-separation dynamics, offering new physical insight into activity-regulated LLPS and suggesting strategies for engineering ATPS morphology using active agents.

Introduction.— Phase separation is a natural phenomenon wherein a homogeneous solution spontaneously segregates into distinct phases. It plays a critical role across diverse fields, including soft matter solutions [1–7], biological cells [8–12], and industrial applications [13–15]. In recent years, liquid–liquid phase separation of aqueous two-phase system (ATPS) has attracted considerable attention [16], particularly due to their roles in forming intracellular compartments [8, 17] and their broad utility in biotechnology [18, 19]. Generally, phase-separated patterns evolve to minimize interfacial free energy through a process called "domain coarsening," wherein the characteristic domain size $\langle \ell \rangle$ grows with time t as $\langle \ell \rangle \propto t^{\nu}$ [20].

While phase separation in passive ATTS has been extensively explored, recent work has increasingly focused on the living control of domain patterns via the introduction of active elements [21–28], such as self-propelled bacteria [29–32]. These motile agents generate hydrodynamic interactions (HIs) as they swim through the fluid [33–36], inducing long-range couplings. It is well established that bacteria can exhibit collective flowing behaviors [37–39] and self-organization [40–42] governed by such HIs. Previous studies have also highlighted that HIs play a crucial role in nonequilibrium phase separation dynamics [24, 43, 44], including the recent observation that active actomyosin-generated flow accelerates the coarsening of lipid membranes [24].

In addition to HIs, wetting-controlled bacterial parti-

tioning may strongly affect phase-separation dynamics. To date, however, previous studies have mainly focused on the partitioning of non-motile colloids [45–48] as well as its influence on coarsening dynamics [49–51]. Recently, Jeong et al. reported a motility-dependent bacterial partitioning in an ATPS of dextran (DEX) and polyethylene glycol (PEG) under a strongly confined setup [31]: while non-motile Bacillus subtilis are confined to the DEX phase, motile Bacillus subtilis can penetrate the soft interfaces and access the PEG phase. Their study reveals that motility-generated forces enable bacteria escape from the weak confinement. Nevertheless, how the addition of bacteria regulates the phase separation dynamics of ATPS remains largely unexplored.

In this Letter, we combine experiments on *Pseudomonas aeruginosa* (*P. aeruginosa*) with fluid particle dynamics (FPD) simulations [52, 53] to elucidate how the interplay between wetting affinity and self-propulsion generates a variety of exotic states in a prototypical ATPS of DEX and PEG. By systematically varying the volume fractions of the DEX phase and *P. aeruginosa*, we uncover a sequence of morphologies, including self-spinning droplets, elongated droplet chains, branched capillary-like clusters, and highly deformed droplets. We find that in the droplet regime, bacterial activity induces autonomous droplet rotation, effectively suppressing domain coarsening compared to systems with non-motile bacteria. Conversely, when the DEX volume fraction

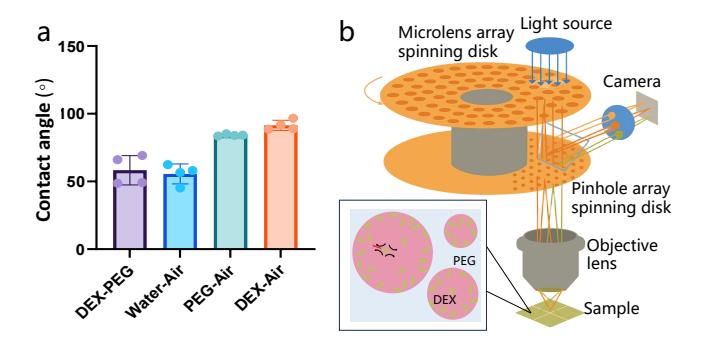


FIG. 1. Interfacial wettability and confocal visualization. (a) Contact angles characterizing the wettability of $P.\ aeruginosa$ across four interfaces: the DEX–PEG–bacteria interface and the water/PEG/DEX–air–bacteria interfaces. (b) Schematic of the spinning-disk confocal microscopy setup used to image the DEX–PEG system containing $P.\ aeruginosa$.

falls below that of the bacteria, a wetting-mediated attraction emerges. This attraction is driven by chemical-potential gradients that direct DEX fluxes toward the bacteria, promoting the formation of capillary bridges between them. Furthermore, dense bacterial partitioning strongly deforms droplet shapes. Our work not only elucidates how motility and wetting together regulate domain evolution, but also establishes a general framework for modeling active agents in ATPS where wetting and hydrodynamic interactions are both critical.

Experimental.—First, to quantify the wetting properties of P. aeruginosa, we measure contact angles by depositing a DEX droplet onto the PEG-bacteria interface (see [54] for details). The contact angle $\theta \approx 50^{\circ}$ provides a direct measure of the wetting affinity and demonstrates that P. aeruginosa are amphiphilic, exhibiting affinity for both the PEG and DEX phases with a slight preference for the DEX phase (Fig. 1(a)). Control experiments were performed by placing water. DEX, and PEG droplets on the air-bacteria interface to determine the respective contact angles. The results indicate that P. aeruginosa show a higher affinity for water compared to PEG and DEX at the air-bacteria interface. This finding demonstrates that the contact angle measured within the ATPS is the more relevant metric for accurately predicting bacterial partitioning.

We then perform experimental observations with a spinning disk confocal microscope (Fig. 1(b)), which enables real-time, three-dimensional (3D) visualization of the phase separation patterns (see [54] for details). Remarkably, we find that even a minimal amount of P. aeruginosa actively reshapes the phase separation behavior, in contrast to the static droplet formation seen in the bacteria-free ATPS (**Movie S1**). Even with a low bacteria volume fraction $\phi_{\text{bac}} = 0.01$, we observe the emergence of exotic and dynamic patterns as the DEX volume fraction ϕ_{dex} was decreased. These structures included self-spinning droplets (Fig. 2(a), top; **Movie S2**),

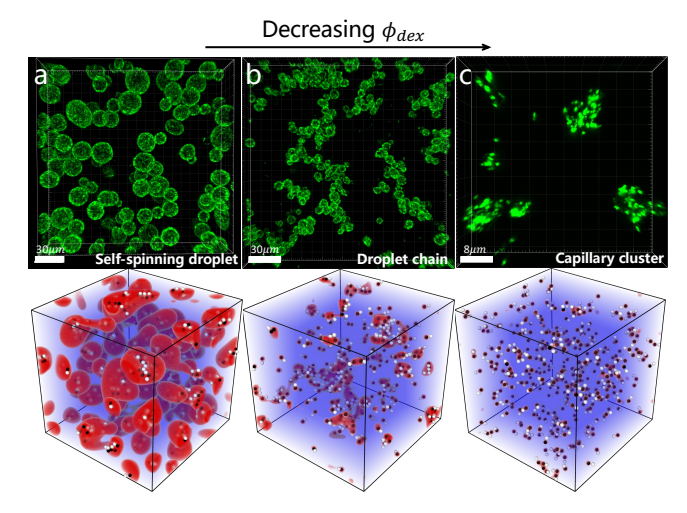


FIG. 2. Morphologies of phase-separated domains in an ATPS with a small amount of P. $aeruginosa~(\phi_{\rm bac}=0.01)$, showing a transition upon decreasing the DEX volume fraction $\phi_{\rm dex}$. (a) Self-spinning droplets at $\phi_{\rm dex}=0.05$. (b) Elongated, interconnected droplet chains at $\phi_{\rm dex}\approx\phi_{\rm bac}$. (c) Branched, capillary-like bacterial clusters at $\phi_{\rm dex}=0.001$. Upper panels: experimental images of green fluorescent protein (GFP)-tagged bacteria. Lower panels: corresponding simulation snapshots (black: head; white: tail; red: DEX phase; blue: PEG phase).

elongated droplet chains (Fig. 2(b), top), and branched bacteria clusters (Fig. 2(c), top). We find the bacteria are primarily distributed at the interfacial region, consistent with their amphiphilic nature as indicated by the contact angle analysis (Fig. 1(a)). The observed non-equilibrium patterns — from self-spinning droplets (Movie S3–S5) to droplet-chain structures (Movie S6) and branched bacteria cluster (Movie S7) — remain robust at higher $\phi_{\rm bac} = 0.05 - 0.1$. Our findings thus establish a robust route for the programmable, living control of domain morphology. Critically, this highly dynamic, bacteria-driven morphological transition represents a phenomenon previously unreported in active matter systems.

Hybrid particle-field simulations.— To gain mechanistic insight into the experimental phenomena, we develop a coarse-grained particle-field hybrid model for simulating active bacteria in a phase-separating binary fluid mixture. Each bacterium is represented as a pusher-type swimmer composed of a head, a tail, and a virtual particle arranged in a rod-like geometry (Fig. S1 in [54]) [40]. Activity is introduced through a force dipole, implemented as an opposing force pair of magnitude f_{act} acting on the tail and the virtual particle. The surrounding binary mixture is described by a Ginzburg-Landau free-energy functional written in terms of a compositional order parameter ψ , where $\psi = 1$ and $\psi = -1$ correspond to the DEX- and PEG-rich phases, respectively. The evolution of ψ follows a conservative advection–diffusion equation coupled to the Navier-Stokes equation, which is solved

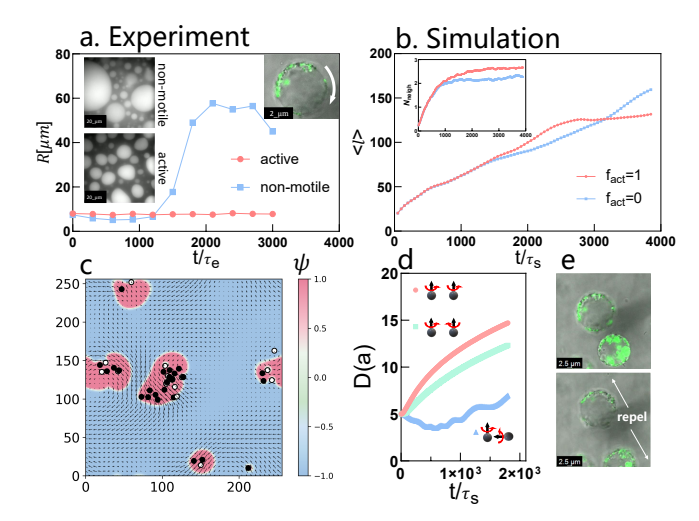


FIG. 3. Dynamic behavior and mechanism of coarsening in self-spinning droplets. (a) Experimental time evolution of the average droplet radius R (time t scaled by $\tau_{\rm e} = \ell_{\rm bac}/v_{\rm bac} \approx$ $0.1 \,\mathrm{s}$, with $\ell_{\mathrm{bac}} \approx 1.5 \,\mu\mathrm{m}$ and $v_{\mathrm{bac}} \approx 15 \,\mu\mathrm{m/s}$) for $\phi_{\mathrm{dex}} = 0.05$ and $\phi_{\text{bac}} = 0.01$. Inset: visual comparison of R for active and non-motile systems at $t = 2400\tau_e$ (left), and a magnified confocal image of a self-spinning droplet (right). (b) Simulated evolution of the domain size $\langle \ell \rangle = 2\pi/\langle q \rangle$, showing suppressed coarsening in the active case. Inset: time evolution of the average neighbor number N_{neigh} . (c) Heat map of the composition field ψ with the velocity field \boldsymbol{v} , demonstrating spontaneous droplet rotation. (d) Simulated centerto-center distance D between two rotating spheres for various rotation orientations, showing effective hydrodynamic repulsion. (e) Experimental time-lapse images showing two selfspinning droplets separating over time without coalescing.

using the FPD method [52, 53, 55]. Wetting interactions between the bacteria and the fluid are incorporated through surface-coupling terms characterized by affinity coefficients γ_1 and γ_2 for the head and tail. Motivated by the experimentally observed amphiphilicity of *P. aeruginosa*, with a slight preference for the DEX phase, we set $\gamma_1 = -4$ and $\gamma_2 = 2$ (see [54] for simulation details).

The simulations qualitatively reproduce the experimentally observed sequence of morphologies as the average composition $\bar{\psi}$ is decreased from $\bar{\psi}=-0.6$ to $\bar{\psi}=-0.9$ and $\bar{\psi}=-0.98$ (Fig. 2, bottom row). This agreement confirms the capability of our model and demonstrates that the observed morphological transitions arise from the coupled effects of activity and wetting affinity.

Self-spinning droplets and hydrodynamic repulsion.— For the droplet-forming regime ($\phi_{\rm dex} > \phi_{\rm bac}$; Fig. 2a), a remarkable observation is the rotation exhibited by isolated DEX-rich droplets. Similar self-spinning droplets have previously been observed for droplets containing dense bacteria [56, 57]. In our case, rotation is driven by the collective propulsion of bacteria primarily distributed at the interfacial region. The rotation of each droplet is a signature of the activity of the encapsulated bacteria. Although our simulations use a much lower bacterial

count than the experiments, the simulated velocity field (Fig. 3(c)) effectively captures the emergent rotational nature surrounding the droplets. This indicates that the rotation is generated by the active forces of randomly oriented bacteria distributed within the droplets, which together create a coherent torque. We find that the rotation increases with decreasing droplet size (smaller $\phi_{\rm dex}$; Movie S3–S5), which is consistent with this interpretation. Further support comes from a control experiment where PEG is set as the minority phase (Fig. A1). We observe static PEG droplets that exhibit minimal rotation due to the low bacterial partitioning into the droplets (Movie S8).

Crucially, we quantify the coarsening dynamics of the self-spinning droplets by tracking the time evolution of the droplet radius R in experiments (see [54] for details). Our experimental data (Fig. 3(a)) reveal that bacterial activity suppresses coarsening, as reflected by a much smaller radius R compared to the case with non-motile bacteria. This indicates a kinetic frustration of droplet coarsening, which is also visualized in the inset of Fig. 3(a), showing a clear difference in droplet size between active and non-motile systems. The activity-induced slowdown in droplet coarsening is also supported by the fact that macroscopic stratification is reached much later in an ATPS with active P. aeruginosa (Fig. A2).

Simulated domain size $\langle \ell \rangle$ based on the ψ -field (Fig. 3(b); see [54] for details) also reveals the same role of activity in suppressing droplet coarsening in the late stage. We also analyze the temporal evolution of the average number of neighboring bacteria $N_{\text{neigh}}(t)$ (the inset of Fig. 3(b)). A previous study has indicated that pushertype bacteria tend to aggregate due to activity [40]. Indeed, N_{neigh} in the active case exceeds the passive counterpart, showing that the activity promotes bacterial aggregation while inhibiting droplet coalescence. We further note that the slowing of droplet growth in the late stages — observed in both active and non-motile systems — can be attributed to the surfactant-like behavior of bacteria residing at the interface (Fig. 2(a)). This is supported by the fact that both systems exhibit slower phase separation compared to a bacteria-free ATPS.

While simulation qualitatively reproduces the experimental trend that activity suppresses late-stage coarsening, discrepancies remain: (1) the early-time plateau and (2) the rapid growth of non-motile droplets seen in experiments (Fig. 3(a)) are absent in simulations. These deviations likely stem from effects not included in our model: mixing-induced transient flows causing (1) and buoyancy-driven convection from the DEX–PEG density mismatch causing (2). Nevertheless, the simulations capture the essential mechanism: activity increases N_{neigh} while inhibiting droplet coalescence in the late stage.

What is the origin of this delayed coarsening among self-spinning droplets? Our simulations of two 3D

rollers (see [54] for details) reveal a hydrodynamic repulsion mechanism (Fig. 3(d)). When two neighboring spheres rotate with appropriate orientations, their center-to-center distance D increases monotonically over time (with Reynolds number $Re \approx 10^{-3}$), demonstrating a purely hydrodynamic, activity-generated repulsion. This behavior is also evident in experimental timelapse imaging (Fig. 3(e); Movie S5, S9), which shows nearby self-spinning droplets separating without coalescing. Whereas macroscopic spinning objects exhibit a repulsive Magnus force only in the nonlinear $(Re \gg 1)$ regime [58], our results demonstrate that an effective dynamic repulsion also emerges at low Reynolds number. This repulsion provides a natural explanation for the suppressed coarsening observed in the active system compared to the non-motile case (Fig. 3(a), Fig. A2).

Transition to droplet-chain morphology.— When the DEX volume fraction becomes comparable to the bacterial volume fraction ($\phi_{\rm dex} \approx \phi_{\rm bac}$), the morphology transitions to a chain-like structure composed of many small, interconnected DEX droplets (Fig. 2(b)). These connected droplets, resembling "colloidal chains," no longer exhibit self-spinning. Our simulations likewise produce chain-like assemblies in which bacteria accumulate at the interfaces and prevent coalescence. Experimentally, this structure emerges when $\phi_{\rm dex} \lesssim \phi_{\rm bac}$, which we attribute to the limited availability of the minority DEX phase. This scarcity forces small droplets to connect, enabling the available DEX to be collectively shared among interfacial bacteria. This regime thus represents a crossover between the self-spinning droplets observed at higher $\phi_{\rm dex}$ (Fig. 2(a)) and the branched clusters that appear when DEX becomes even more limited (Fig. 2(c)).

Wetting-mediated attraction and branched clusters.— When the DEX volume fraction becomes smaller than the bacterial volume fraction ($\phi_{\rm dex} < \phi_{\rm bac}$), the system enters a regime dominated by wetting-mediated attraction, leading to the formation of capillary bridges between bacteria (Fig. 2(c)). Notably, analysis of the phase-separation kinetics reveals a reversal in the role of activity: motility now accelerates domain coarsening. The experimentally measured cluster area A is significantly larger under active conditions than for nonmotile bacteria, indicating faster coarsening in the presence of activity (Fig. 4(a)). Our simulations reproduce this trend in the low-DEX-fraction regime ($\bar{\psi} = -0.98$; Fig. 4(b)). At such small ϕ_{dex} , the extent of bacterial aggregation correlates directly with domain growth. Indeed, the consistently higher $N_{\text{neigh}}(t)$ in the active case (inset of Fig. 4(b)) confirms that motility enhances bacterial aggregation, thereby driving faster coarsening.

The microscopic mechanism underlying this regime is clarified by two-bacteria simulations ($\bar{\psi}=-0.98$; Fig. 4(c)). Whereas affinity-less bacteria show no attraction — and may even experience slight hydrodynamic repulsion — introducing affinity for the DEX phase pro-

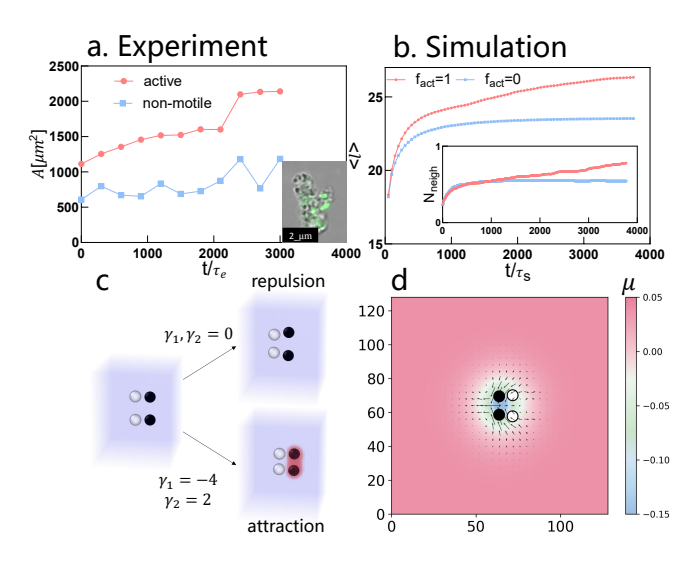


FIG. 4. Dynamic behavior and mechanism of branched bacterial clusters. (a) Experimental time evolution of the DEX-phase cluster area A for $\phi_{\rm dex}=0.001$ and $\phi_{\rm bac}=0.01$, showing accelerated phase-separation kinetics under activity. Inset: magnified confocal image of a branched bacterial cluster. (b) Simulated evolution of the ψ -based domain size $\langle \ell \rangle$, confirming faster coarsening for $f_{\rm act}=1$ compared with $f_{\rm act}=0$. Inset: time evolution of the average neighbor number $N_{\rm neigh}$. (c) Two-bacterium simulation showing that attractive interactions arise only when wetting affinity is present ($\gamma_1=-4$, $\gamma_2=2$); without affinity, no attraction is observed. (d) Heat map of the chemical potential μ overlaid with the velocity field v, revealing solvent fluxes directed toward the inter-bacterial region that forms a capillary bridge.

duces a strong attraction that stabilizes a bacterial pair. Examination of the chemical-potential field μ and velocity field v (Fig. 4(d)) reveals solvent fluxes directed toward the inter-bacterial region, driven by chemical-potential gradients. This wetting-induced attraction promotes branched bacterial aggregation and defines a regime in which active propulsion enhances coarsening. The mechanism, arising from spatially varying chemical potential, closely parallels wetting-induced attractions previously observed between colloids [50, 51]. More broadly, it may help explain bacterial aggregation phenomena [32, 59, 60] and suggests a strategy for controlling aggregation by introducing a small amount of a preferentially wetting phase.

Active deformation of droplets.— We finally discuss the impact of bacterial concentration on droplet morphology. As the bacterial volume fraction increases to $\phi_{\rm bac}=0.1$, many droplets become strongly deformed (Fig. A3). This deformation reflects a competition between interfacial tension, which favors spherical shapes, and active forces generated by the bacteria, which distort the interface. At high $\phi_{\rm bac}$, active stresses outpace interfacial relaxation, producing highly irregular, fingerlike morphologies. Similar actively deformed droplets have been reported in previous studies [61, 62]. The observed

deformation also suggests a potential route to network formation, as elongated droplets can more readily percolate than spherical ones.

Activity-enhanced escape under weak wetting affinity.— To further demonstrate the generality of our approach, we conducted simulations with a low wetting affinity ($\gamma_1 = \gamma_2 = -0.5$, corresponding to very weak attraction to the DEX phase). In this case, increasing bacterial activity promotes escape from the DEX-rich phase (Fig. A4), consistent with recent observations of activity-dependent partitioning [31]. These results underscore that our framework is broadly applicable for simulating active particles [63, 64] in ATPS, where wetting, activity, and HIs all play essential roles.

Summary. — In summary, we combine experiments and fluid particle dynamics simulations to investigate how the addition of P. aeruginosa modulates phase-separation dynamics in a binary DEX-PEG mixture. By tuning the DEX volume fraction $\phi_{\rm dex}$ and bacterial volume fraction $\phi_{\rm bac}$, we uncover a sequence of exotic morphologies: (i) self-spinning droplets driven by bacterial activity and stabilized by hydrodynamic repulsion when $\phi_{\rm dex} > \phi_{\rm bac}$; (ii) elongated droplet chains emerging when $\phi_{\rm dex} \approx \phi_{\rm bac}$, where limited DEX content must be shared among interfacial bacteria; (iii) branched, capillary-like bacterial clusters driven by wetting-mediated attraction when $\phi_{\text{dex}} < \phi_{\text{bac}}$; and (iv) strongly deformed, fingerlike droplets at high bacterial concentrations due to activityinduced stresses. Activity produces a dual kinetic effect — suppressing coarsening through flow-induced repulsion in the self-spinning droplet regime, but accelerating it in the capillary-cluster regime due to enhanced aggregation driven by chemical-potential gradients. Collectively, our results show that active bacteria enable living control of ATPS via the coupled effects of activity and wetting. These findings deepen our fundamental understanding of active phase separation and suggest practical strategies for designing stable emulsions and manipulating bacterial aggregation by introducing a small amount of a preferentially wetting phase.

We thank Huihui Liu for performing part of the bacteria experiments and Tianyi Zhang for contributing to the implementation of the simulation code. J.Y. acknowledges support from the startup fund of HKUST(GZ) and the National Natural Science Foundation of China (Grant No. 22503076). H.T. is supported by the Grant-in-Aid for Specially Promoted Research (JSPS KAKENHI Grant No. JP20H05619). C.W. acknowledges support from the Science and Technology Development Fund, Macao SAR (FDCT, No. 0001/2021/AKP, 0024/2023/AFJ, 0209/2024/AGJ, 0031/2023/ITP1, and 005/2023/SKL); the National Natural Science Foundation of China (Grant Nos. 32361163656, 32022088, 32230056); the University of Macau (MYRG-GRG2023-00136-ICMS-UMDF, MYRG-

GRG2024-00189-ICMS-UMDF, and MYRG-CRG2023-00009-IAPME); and the Zhuhai UM Science & Technology Research Institute (CP-102-2024). Simulations were performed on the HPC platform at HKUST(GZ).

End Matter

Additional characterization.— The End Matter presents additional results on the phase separation of a DEX-PEG binary mixture containing P. aeruginosa. Figure A1 investigates the system under conditions of a high DEX volume fraction $\phi_{\rm dex} = 0.6$ and a bacterial volume fraction $\phi_{\rm bac} = 0.05$. Both the experimental results and simulations reveal that the PEG droplets remain spherical and exhibit no rotation. When bacteria are confined to the continuous DEX-rich phase at this high $\phi_{\rm dex}$, the active forces exerted near the interface are insufficient to induce self-spinning of PEG-rich droplets. This provides evidence supporting the mechanism that active forces from bacteria inside the droplets are critical for driving the rotation.

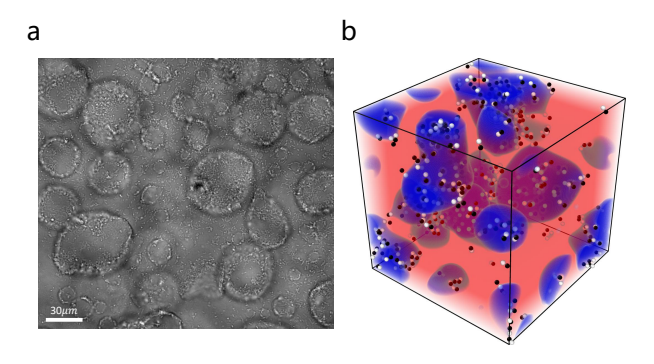


FIG. A1. Phase separation under $\phi_{\text{dex}} = 0.6$ and $\phi_{\text{bac}} = 0.05$. (a) Brightfield microscopy image showing spherical PEG droplets that exhibit no rotation. (b) Corresponding simulation in which *P. aeruginosa* populate the DEX phase, producing similarly stationary PEG droplets.

We compare the macroscopic phase separation of an ATPS containing active versus non-motile *P. aeruginosa* (Figure A2). The non-motile systems exhibit complete macroscopic stratification (clear separation into two distinct bulk layers) after approximately 30 minutes. In contrast, the active systems remain stable and visibly mixed for a significantly longer duration, up to 2 hours. This finding provides evidence that bacterial activity acts as a potent inhibitor of macroscopic phase separation. By counteracting the dynamic processes of droplet coarsening, active bacteria enhance the stability of the emulsion.

Figure A3 explores the active deformation of DEX-rich droplets as the bacterial volume fraction $\phi_{\rm bac}$ increases. Experimentally, DEX-rich droplets show elongated, fingerlike morphology ($\phi_{\rm bac}=0.05$) and highly irregular shape ($\phi_{\rm bac}=0.1$). This behavior is corroborated by simulations. Collectively, this implies that the active forces originating from the bacteria within the droplet surpass the surface tension forces—the factor favoring

After 30 minutes



After 2 hours



FIG. A2. Macroscopic phase separation in ATPS containing active (left) and non-motile (right) P. aeruginosa at $\phi_{\rm bac} = 0.05$. The DEX volume fraction $\phi_{\rm dex}$ increases from left to right (0.08, 0.16, 0.32). After 30 minutes, non-motile systems exhibit complete macroscopic stratification, whereas active systems remain mixed and stable for up to 2 hours.

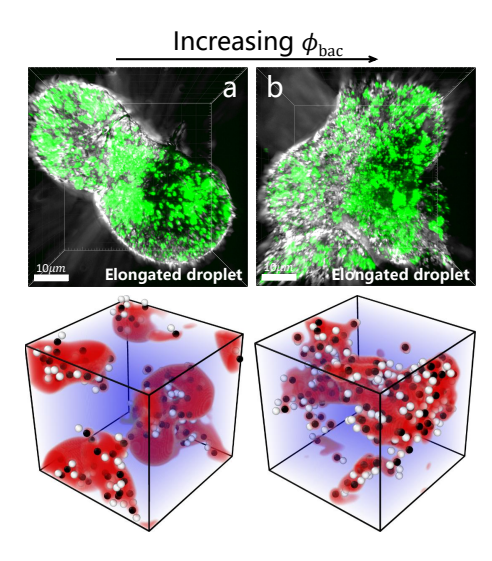


FIG. A3. Droplet deformation driven by increasing bacterial volume fraction at $\phi_{\rm dex}=0.2$. (a) Elongated, fingerlike droplet at $\phi_{\rm bac}=0.05$. (b) Highly irregular droplet at $\phi_{\rm bac}=0.1$. Bottom row: simulations at $\phi_{\rm bac}=0.025-0.05$ qualitatively reproducing the increasing deformation with higher bacterial concentration.

sphericity—leading to the pronounced deformation.

We also perform simulations to investigate the activity-dependent partitioning of bacteria that exhibit a weak wetting affinity for the DEX phase (Figure A4). While non-motile bacteria remain confined to the DEX phase ($\alpha_{\rm in} \approx 1$) during the phase separation process, the introduction of activity substantially increases the fraction of bacteria that escape the DEX phase. This result demonstrates that bacterial activity can overcome thermodynamic partitioning tendencies governed by wetting

Increasing activity

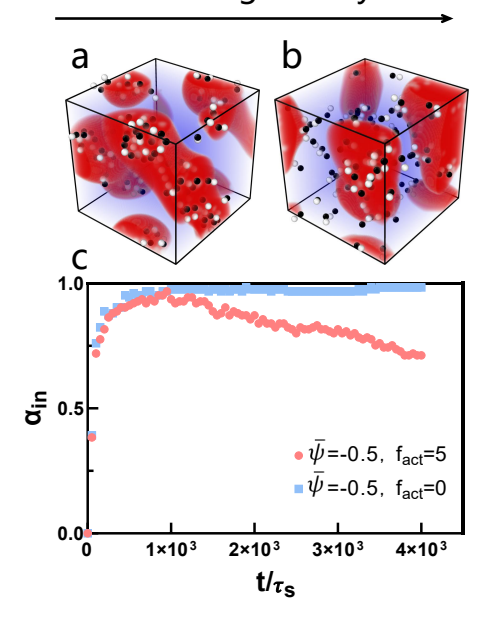


FIG. A4. Activity-enhanced escape of bacteria. Simulations examining activity-dependent partitioning at $\bar{\psi}=-0.5$ and $\gamma_1=\gamma_2=-0.5$. (a) Passive case $(f_{\rm act}=0)$: bacteria remain predominantly in the DEX-rich phase. (b) Active case $(f_{\rm act}=5)$: a significant fraction of bacteria escape from the DEX-rich phase. (c) Time evolution of the fraction of bacteria in the DEX-rich phase, $\alpha_{\rm in}$ (see [54]). Activity causes a clear decrease in $\alpha_{\rm in}$, consistent with recent observations of activity-enabled escape [31].

effects [31].

- * These authors contributed equally
- † cmwang@um.edu.mo
- [‡] tanaka@iis.u-tokyo.ac.jp
- § jiaxingyuan@hkust-gz.edu.cn
- [1] Masao Doi, *Soft matter physics* (Oxford University Press, 2013).
- [2] Hajime Tanaka, "Unusual phase separation in a polymer solution caused by asymmetric molecular dynamics," Phys. Rev. Lett. 71, 3158–3161 (1993).
- [3] A. E. Bailey, W. C. K. Poon, R. J. Christianson, A. B. Schofield, U. Gasser, V. Prasad, S. Manley, P. N. Segre, L. Cipelletti, W. V. Meyer, M. P. Doherty, S. Sankaran, A. L. Jankovsky, W. L. Shiley, J. P. Bowen, J. C. Eggers, C. Kurta, T. Lorik, P. N. Pusey, and D. A. Weitz, "Spinodal decomposition in a model colloid-polymer mixture in microgravity," Phys. Rev. Lett. 99, 205701 (2007).
- [4] Hajime Tanaka, "Viscoelastic phase separation in soft matter and foods," Faraday Discuss. 158, 371–406 (2012).
- [5] Michio Tateno and Hajime Tanaka, "Power-law coarsening in network-forming phase separation governed by mechanical relaxation," Nat. Commun. 12, 912 (2021).
- [6] Jiaxing Yuan, Michio Tateno, and Hajime Tanaka, "Me-

- chanical slowing down of network-forming phase separation of polymer solutions," ACS Nano 17, 18025–18036 (2023).
- [7] Shensheng Chen and Zhen-Gang Wang, "Charge asymmetry suppresses coarsening dynamics in polyelectrolyte complex coacervation," Phys. Rev. Lett. 131, 218201 (2023).
- [8] Clifford P. Brangwynne, Christian R. Eckmann, David S. Courson, Agata Rybarska, Carsten Hoege, Jöbin Gharakhani, Frank Jülicher, and Anthony A. Hyman, "Germline P granules are liquid droplets that localize by controlled dissolution/condensation," Science 324, 1729–1732 (2009).
- [9] Pilong Li, Sudeep Banjade, Hui-Chun Cheng, Soyeon Kim, Baoyu Chen, Liang Guo, Marc Llaguno, Javoris V Hollingsworth, David S King, Salman F Banani, et al., "Phase transitions in the assembly of multivalent signalling proteins," Nature 483, 336–340 (2012).
- [10] Simon Alberti, Amy Gladfelter, and Tanja Mittag, "Considerations and challenges in studying liquid-liquid phase separation and biomolecular condensates," Cell 176, 419–434 (2019).
- [11] Sarah L. Perry, "Phase separation: Bridging polymer physics and biology," Curr. Opin. Colloid Interface Sci. 39, 86–97 (2019).
- [12] Hajime Tanaka, "Viscoelastic phase separation in biological cells," Commun. Phys. 5, 167 (2022).
- [13] Hajime Tanaka, "Formation of network and cellular structures by viscoelastic phase separation," Adv. Mater. 21, 1872–1880 (2009).
- [14] C. Gallegos and J.M. Franco, "Rheology of food, cosmetics and pharmaceuticals," Curr. Opin. Colloid Interface Sci. 4, 288–293 (1999).
- [15] Fei Wang, Patrick Altschuh, Lorenz Ratke, Haodong Zhang, Michael Selzer, and Britta Nestler, "Progress report on phase separation in polymer solutions," Adv. Mater. 31, 1806733 (2019).
- [16] Xunan Zhang, Mingxue Han, Shuang Han, and Wei Zong, "Aqueous two-phase system (ATPS): from basic science to applications," RSC advances 15, 9041–9054 (2025).
- [17] Anthony A Hyman, Christoph A Weber, and Frank Jülicher, "Liquid-liquid phase separation in biology," Annu. Rev. Cell Dev. Biol. 30, 39–58 (2014).
- [18] Alyne G Teixeira, Rishima Agarwal, Kristin Robin Ko, Jessica Grant-Burt, Brendan M Leung, and John P Frampton, "Emerging biotechnology applications of aqueous two-phase systems," Adv. Healthc. Mater. 7, 1701036 (2018).
- [19] Qingming Ma, Yang Song, Wentao Sun, Jie Cao, Hao Yuan, Xinyu Wang, Yong Sun, and Ho Cheung Shum, "Cell-inspired all-aqueous microfluidics: from intracellular liquid-liquid phase separation toward advanced biomaterials," Adv. Sci. 7, 1903359 (2020).
- [20] Akira Onuki, *Phase transition dynamics* (Cambridge University Press, 2002).
- [21] Joakim Stenhammar, Raphael Wittkowski, Davide Marenduzzo, and Michael E. Cates, "Activity-induced phase separation and self-assembly in mixtures of active and passive particles," Phys. Rev. Lett. 114, 018301 (2015).
- [22] Jan Smrek and Kurt Kremer, "Small activity differences drive phase separation in active-passive polymer mixtures," Phys. Rev. Lett. 118, 098002 (2017).

- [23] Jie Zhang, Ricard Alert, Jing Yan, Ned S Wingreen, and Steve Granick, "Active phase separation by turning towards regions of higher density," Nat. Phys. 17, 961–967 (2021).
- [24] Daniel P. Arnold, Aakanksha Gubbala, and Sho C. Takatori, "Active surface flows accelerate the coarsening of lipid membrane domains," Phys. Rev. Lett. 131, 128402 (2023).
- [25] Saraswat Bhattacharyya and Julia M. Yeomans, "Phase separation driven by active flows," Phys. Rev. Lett. 130, 238201 (2023).
- [26] Jiaxing Yuan and Hajime Tanaka, "Colloid phase separation dynamics driven by chiral turbulent flows," Phys. Rev. Res. 6, 023186 (2024).
- [27] Etienne Jambon-Puillet, Andrea Testa, Charlotta Lorenz, Robert W Style, Aleksander A Rebane, and Eric R Dufresne, "Phase-separated droplets swim to their dissolution," Nat. Commun. 15, 3919 (2024).
- [28] Siwen Sun, Jianhong Wang, Yudong Li, Alexander B Cook, Bingbing Sun, Sebastian Novosedlik, Lars JMM Paffen, Sander GAM Huisman, Lou MV Raeven, Alexander D Fusi, et al., "Engineering motile coacervate droplets via nanomotor stabilization," J. Am. Chem. Soc. 147, 31871–31881 (2025).
- [29] Daniel Grober, Ivan Palaia, Mehmet Can Uçar, Edouard Hannezo, Andela Šarić, and Jérémie Palacci, "Unconventional colloidal aggregation in chiral bacterial baths," Nat. Phys. 19, 1680–1688 (2023).
- [30] Luhui Ning, Xin Lou, Qili Ma, Yaochen Yang, Nan Luo, Ke Chen, Fanlong Meng, Xin Zhou, Mingcheng Yang, and Yi Peng, "Hydrodynamics-induced long-range attraction between plates in bacterial suspensions," Phys. Rev. Lett. 131, 158301 (2023).
- [31] Jiyong Cheon, Kyu Hwan Choi, Kevin J. Modica, Robert J. Mitchell, Sho C. Takatori, and Joonwoo Jeong, "Motility modulates the partitioning of bacteria in aqueous two-phase systems," Phys. Rev. Lett. 135, 128401 (2025).
- [32] Matthew E Black, Chenyi Fei, Ricard Alert, Ned S Wingreen, and Joshua W Shaevitz, "Capillary interactions drive the self-organization of bacterial colonies," Nat. Phys., 1–7 (2025).
- [33] Knut Drescher, Jörn Dunkel, Luis H Cisneros, Sujoy Ganguly, and Raymond E Goldstein, "Fluid dynamics and noise in bacterial cell-cell and cell-surface scattering," Proc. Natl. Acad. Sci. U.S.A. 108, 10940–10945 (2011).
- [34] Julia M Yeomans, Dmitri O Pushkin, and Henry Shum, "An introduction to the hydrodynamics of swimming microorganisms," Eur. Phys. J. Special Topics 223, 1771– 1785 (2014).
- [35] Jinglei Hu, Mingcheng Yang, Gerhard Gompper, and Roland G Winkler, "Modelling the mechanics and hydrodynamics of swimming E. coli," Soft matter 11, 7867– 7876 (2015).
- [36] M Reza Shaebani, Adam Wysocki, Roland G Winkler, Gerhard Gompper, and Heiko Rieger, "Computational models for active matter," Nat. Rev. Phys. 2, 181–199 (2020).
- [37] Kun-Ta Wu, Jean Bernard Hishamunda, Daniel TN Chen, Stephen J DeCamp, Ya-Wen Chang, Alberto Fernández-Nieves, Seth Fraden, and Zvonimir Dogic, "Transition from turbulent to coherent flows in confined three-dimensional active fluids." Science 355, eaal1979

- (2017).
- [38] Haoran Xu, Justas Dauparas, Debasish Das, Eric Lauga, and Yilin Wu, "Self-organization of swimmers drives long-range fluid transport in bacterial colonies," Nat. Commun. 10, 1792 (2019).
- [39] He Li, Hugues Chaté, Masaki Sano, Xia-qing Shi, and HP Zhang, "Robust edge flows in swarming bacterial colonies," Phys. Rev. X 14, 041006 (2024).
- [40] Akira Furukawa, Davide Marenduzzo, and Michael E Cates, "Activity-induced clustering in model dumbbell swimmers: The role of hydrodynamic interactions," Phys. Rev. E 90, 022303 (2014).
- [41] Xiao Chen, Xiang Yang, Mingcheng Yang, and HP Zhang, "Dynamic clustering in suspension of motile bacteria," Europhys. Lett. 111, 54002 (2015).
- [42] Mario Theers, Elmar Westphal, Kai Qi, Roland G Winkler, and Gerhard Gompper, "Clustering of microswimmers: interplay of shape and hydrodynamics," Soft Matter 14, 8590–8603 (2018).
- [43] Hajime Tanaka, "Viscoelastic model of phase separation," Phys. Rev. E 56, 4451 (1997).
- [44] Hajime Tanaka, "Phase separation in soft matter: The concept of dynamic asymmetry," Soft Interfaces: Lecture Notes of the Les Houches Summer School 98, 465–526 (2017).
- [45] HT Dobbs and JM Yeomans, "Capillary condensation and prewetting between spheres," J. Phys.: Condens. Matter 4, 10133 (1992).
- [46] Daniel Bonn, Jens Eggers, Joseph Indekeu, Jacques Meunier, and Etienne Rolley, "Wetting and spreading," Rev. Mod. Phys. 81, 739–805 (2009).
- [47] Job HJ Thijssen and Paul S Clegg, "Demixing, remixing and cellular networks in binary liquids containing colloidal particles," Soft Matter 6, 1182–1190 (2010).
- [48] Haodong Zhang, Hongmin Zhang, Fei Wang, and Britta Nestler, "Wetting effect induced depletion and adsorption layers: Diffuse interface perspective," ChemPhysChem 25, e202400086 (2024).
- [49] Hajime Tanaka, "Interplay between wetting and phase separation in binary fluid mixtures: roles of hydrodynamics," J. Phys.: Condens. Matter 13, 4637 (2001).
- [50] Takeaki Araki and Hajime Tanaka, "Dynamic depletion attraction between colloids suspended in a phaseseparating binary liquid mixture," J. Condens. Matter Phys. 20, 072101 (2008).
- [51] Takeaki Araki and Hajime Tanaka, "Wetting-induced depletion interaction between particles in a phase-

- separating liquid mixture," Phys. Rev. E 73, 061506 (2006).
- [52] Hajime Tanaka and Takeaki Araki, "Simulation method of colloidal suspensions with hydrodynamic interactions: Fluid particle dynamics," Phys. Rev. Lett. 85, 1338–1341 (2000).
- [53] Akira Furukawa, Michio Tateno, and Hajime Tanaka, "Physical foundation of the fluid particle dynamics method for colloid dynamics simulation," Soft Matter 14, 3738–3747 (2018).
- [54] See Supplemental Material at http://link.aps.org/supplemental/xxx on the details of experiments and simulations.
- [55] Francis H. Harlow and J. Eddie Welch, "Numerical calculation of time-dependent viscous incompressible flow of fluid with free surface," Phys. Fluids 8, 2182–2189 (1965).
- [56] Gabriel Ramos, María Luisa Cordero, and Rodrigo Soto, "Bacteria driving droplets," Soft Matter 16, 1359–1365 (2020).
- [57] Mojtaba Rajabi, Hend Baza, Taras Turiv, and Oleg D Lavrentovich, "Directional self-locomotion of active droplets enabled by nematic environment," Nat. Phys. 17, 260–266 (2021).
- [58] Yusuke Goto and Hajime Tanaka, "Purely hydrodynamic ordering of rotating disks at a finite reynolds number," Nat. Commun. 6, 5994 (2015).
- [59] Gavin Melaugh, Jaime Hutchison, Kasper Nørskov Kragh, Yasuhiko Irie, Aled Roberts, Thomas Bjarnsholt, Stephen P Diggle, Vernita D Gordon, and Rosalind J Allen, "Shaping the growth behaviour of biofilms initiated from bacterial aggregates," PloS one 11, e0149683 (2016).
- [60] Catherine R Armbruster and Matthew R Parsek, "New insight into the early stages of biofilm formation," Proc. Natl. Acad. Sci. U.S.A. 115, 4317–4319 (2018).
- [61] Liam J Ruske and Julia M Yeomans, "Morphology of active deformable 3D droplets," Phys. Rev. X 11, 021001 (2021).
- [62] Sho Kawakami and Petia M Vlahovska, "Migration and deformation of a droplet enclosing an active particle," J. Fluid Mech. 1007, A41 (2025).
- [63] Jie Zhang, Erik Luijten, Bartosz A Grzybowski, and Steve Granick, "Active colloids with collective mobility status and research opportunities," Chem. Soc. Rev. 46, 5551–5569 (2017).
- [64] Solon Alexandre and Zhao Yongfeng, "The surprising physics of interfaces in active matter," Chin. Phys. Lett. 42, 100901–100901 (2025).